

Discontinuity detection on industrial parts : real-time image segmentation using Parzen's Kernel.

Johel Mitéran¹, Sophie Kohler², Pierre Geveaux^{2*}, Patrick Gorria², Jiri Matas³

¹ Laboratoire Le2i
Université de Bourgogne
Aile des sciences de l'ingénieur
21078 –Dijon
France

² Laboratoire Le2i
Université de Bourgogne
IUT Le Creusot
12 rue de la fonderie
71200 Le Creusot - FRANCE

³ Center of Machine Perception
CTU Prague
Karlovo nam. 13
12135
Czech Republic

* Scholarship of the Burgundy Regional Council

E-mail : miteranj@u-bourgogne.fr
{p.geveaux, sophie,Patrick.Gorria}@iutlecreusot.u-bourgogne.fr
matas@cmp.felk.cvut.cz

Abstract.

The paper describes a real-time system for visual inspection of textured industrial parts - CRT cathodes. Four types of anomalies are detected: smooth surfaces, bumps, missing material and hollow knocked surfaces. In order to distinguish defective and acceptable zones with minimum error, both optimal lighting parameters and most discriminative features are selected. The feature and lighting selection process is based on probability density estimation method using a Parzen's kernel based technique. This same method is used in a multi dimensional way to perform the pixel-wise segmentation step, based on the Bayes rule. The nature of the application requires a real-time response. The segmentation is therefore implemented as a hyperrectangle based method of feature space division. A comparison of the two classifiers behavior is presented. The final cathode classification step is performed using the segmented image combined with a circularity inspection of the part. The proposed approach achieved the quality required. The system runs in real-time on a standard, mid-range PC. Since the proposed approach does not take into account any particular features of the inspected part, e.g its shape, it can be used in other visual inspection tasks of textured parts.

Key words : textured image, Parzen kernel, hyperrectangle, segmentation, classification, real time processing, multithreaded implementation.

Introduction

In this paper, a complete real-time system for detection and classification of certain anomalies of CRT cathodes is presented. Defects of the emissive part of the cathode (diameter: 2mm), which is critical for the final tube quality, influence the textured appearance of the cathode surface. Therefore, it is possible to automatically detect the anomalies using machine vision. Currently, the inspection is performed manually by trained operators at a high cost. Productivity increase is therefore the primary goal of the presented work. The manufacturer's specification require the speed of at least ten inspections per second. The quality of the produced parts must be maintained at least at the current level.

In this machine vision application, two problems are addressed. Firstly: the area covered by anomalies must be localised (segmented). In a second step, the defective part is analysed and classified. The success of these two steps depends on three critical design decisions - 1. The set-up of the image acquisition system; - 2. The choice of texture descriptors (features) used and 3. The defect segmentation and classification procedure. In the proposed system, the first two problems are addressed together. This joint optimisation of light and camera position together with texture feature selection is presented in detail by (Geveaux et al., 2000). We only give a brief overview of this selection, necessary for understanding the rest of the paper that focuses on the design of the defect classification system, compares two classification methods used in order to respect real-time constraints, and presents results obtained on a large test set and the real-time implementation of the control.

The defective areas and defect-free areas can be described using any of the large number of texture descriptors proposed in the literature. Methods based on measurements of local frequency variations, defining a neighborhood around the considered pixel, and an operator in this neighborhood, are among the most popular (Coquerez and Phillip, 1995, Unser, 1986). The feature selection and the lighting and acquisition system are summarised in the following section.

Segmentation is widely described in image processing literature. Many different methods could be applied in our application, from Markov random field or active contour methods (snakes), for example, to simple pixel-wise classification. Mainly because of the time constraint (10 images/s, size 300x300), only segmentation methods based on context-free local analysis of pixel neighbourhoods were considered. Classification is a central problem of pattern recognition (Duda and Hart, 1973) and many approaches to the problem have been proposed, e.g. neural networks (Bishop, 1995), Support Vector Machines (Vapnik, 1998), k-nearest neighbours and kernel-based methods to name the most common. The chosen classifier must either be implemented in low-cost hardware or in optimised software running in real-time.

We studied two supervised classification methods in order to perform the segmentation step. The first approach is based on the estimation of the probability density function of each class using a kernel-based method (Parzen's kernel) followed by a Bayes decision rule. The second method divides the feature space into a set of hyperrectangles, for which simple comparators may easily verify the membership condition (Miteran et al., 1994, 1997). The segmentation step is described in the second part of this paper.

In the last part, we present the last step of the inspection task: the cathode classification, using the segmented image and an inspection of the part shape circularity, which avoids border artifacts. The implementation of the algorithm using multithreading programming is described, and results of our real-time quality control system, applied on a large set of textured images, are presented.

DEFECT LOCALISATION. LIGHTING AND SEGMENTATION FEATURES SELECTION

Defect localisation

In the application, four types of anomalies of cathodes should be detected: bump ("Bump"), smooth surface ("Smooth"), missing material ("Missing") and hollow knocked surface ("Hollow"). Examples of images with anomalies are depicted in Figure 1. The anomalies show significant variation of size and appearance. It seems there is no simple decision strategy that would allow defect recognition using a priori knowledge. Therefore, the recognition system must be trained on data provided by an experienced human expert. The expert choice of representative anomalies is based on visual inspection using a binocular microscope. In all, 500 cathodes were chosen for training and test.

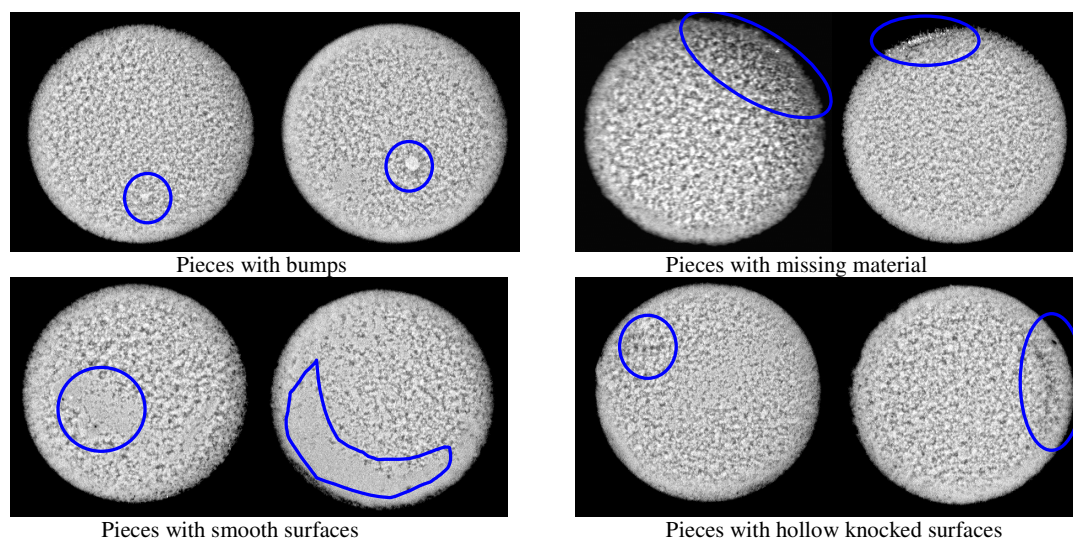


Figure 1 : Samples of anomalies to be detected

Training of a classifier requires labeled samples: examples of defective areas and some positive examples, i.e. defect-free areas. For example, the bottom left image in Figure 2 shows the area labeled "Smooth", and the bottom right image shows defect free pixels.

The available data are split into training and test sets. The training set is used in learning stage whereas test data are used for independent performance evaluation. The training set contains, for each lighting system, 80 images, 16 for each type of defect and 16 defect-free. From each image, 1000 pixels are randomly chosen from the region labeled by the expert.

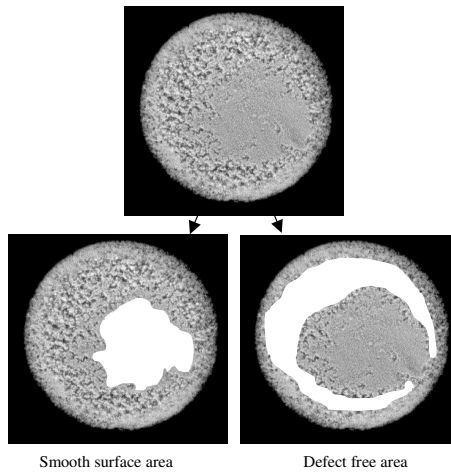


Figure 2 : A selection of defective areas and acceptable areas

Lighting and segmentation features selection

Good choice of lighting is important in most visual inspection problems (Batchelor, 1985). Typically, the lighting system is set up ad hoc, e.g. to make the anomalies to be detected visible to human observers. The discriminative power of lighting and segmentation features is considered independently. In this study, the lighting and feature selection are optimised jointly using a method described in details by Geveaux et al. (2000). We recall here the principle and the results used in the final classification step.

Geveaux developed a method based on the measurement of discriminative power of each feature, using an estimate of the probability density function of each class of pixel (C_n : flaw class and C_f : defect free class), for each feature. He showed that the error E_{nf} between C_n and C_f in a given description space D can be overestimated by the sum on each class of defect of the minimum error on features. The error on each feature between class C_1 and C_2 depends on the probability density function estimated using a Parzen kernel based method (Duda and Hart, 1973), described in the second part of this paper. That means that the efficiency of each feature, for a given lighting, can be estimated by the overlap of both density probability functions obtained from the selected areas. The smaller the overlap, the higher the discrimination power of the feature for a given lighting.

Marginal densities are computed on a set of a priori features for a set of samples and for each lighting device. Then the upper bound of the E_{nf} error is used to choose a suitable lighting system and an appropriate subset of descriptive features. In our experiments, we tested a set of 15 lighting systems (some of them were "manually" removed, given clearly too poor information to be exploited), and a set of 122 segmentation features, computed in various sizes of neighborhood. This pre-selection of features has to be made according to the knowledge and the appearance of anomalies (Coquerez and Phillip, 1995, Lin and Michael, 1973). For instance, applied to our industrial application, the local contrast and the local mean of the Roberts gradient seem to be interesting features for the characterisation of smooth surfaces. The defect free areas present a very different contrast and a different gradient density compared to a smooth surface.

The complete set consists of simple morphological filters (erosion, dilatation, open, close, ...), filters based on histogram measurements and transformations (max-min filters, moments...). The computation cost played an important role in the choice of local operators considered in the feature selection, since the complete segmentation time should be performed in less than 100 ms.

After the selection of features giving the smallest overlaps, the next step consists of analyzing the redundancy of these features through the computation of the correlation coefficient. This enables us to reduce the number of features required to detect all types of anomalies.

The selected lighting system

Applying our method on the test set, we choose a lighting system based on a ring of L.E.D. presented on Figure 3.

Fortunately, independently from the feature selection, an L.E.D. lighting system is very well suited to fast industrial control, since the L.E.D. may be operated in a flash mode, increasing the lighting power during acquisition. The life time of such L.E.D. is significantly higher than for many other lighting devices, which is important in the envisaged application. However, the discrete structure of the device could be seen as a problem for the lighting homogeneity and then for the robustness of the defect detection against part rotation, for example. In order to help the user to adjust the device, we developed a software for measuring the lighting homogeneity and intensity, and we built a theoretical model of this lighting device (Aluze et al., 1997, Geveaux, 2000), allowing the user to choose the best adjustment (distance between the ring centre and the part centre, direction of each L.E.D.,

etc.). Moreover, an important study of repeatability achieved by the company involved in this project shows that the set of lighting and measurement is sufficiently robust against size variation of the part and rotation of the part.

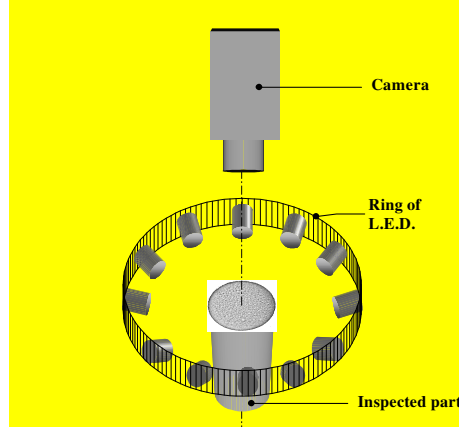


Figure 3 : Lighting system

The selected features

As detailed by Geveaux et al. (2000), the local mean of pixel luminance, the local mean of the Roberts gradient and the local contrast, computed in a $[12 \times 12]$ neighbourhood, have been selected to bring out the four types of anomalies. An example of these features is presented on Figure 4.

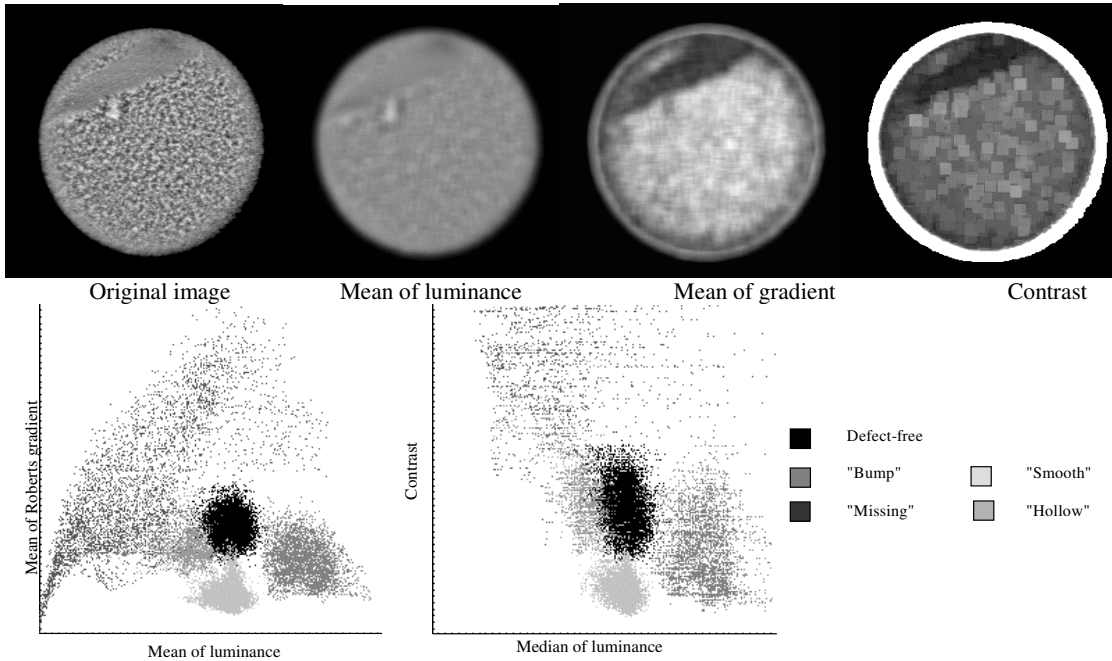


Figure 4 : Example of extracted features and representation of sampling in this features space

The local contrast $V(i,j)$ in an $[n \times m]$ neighborhood of pixel $A(i,j)$ can be expressed as follows:

$$(1) \quad V(i, j) = \frac{A_{\max} - A_{\min}}{A_{\max} + A_{\min}}$$

with

$$(2) \quad A_{\max} = \max \left\{ A(i+k, j+l), -\left\lfloor \frac{n-1}{2} \right\rfloor \leq k \leq \left\lfloor \frac{n}{2} \right\rfloor, -\left\lfloor \frac{m-1}{2} \right\rfloor \leq l \leq \left\lfloor \frac{m}{2} \right\rfloor \right\}, \quad A_{\min} = \min \left\{ A(i+k, j+l), -\left\lfloor \frac{n-1}{2} \right\rfloor \leq k \leq \left\lfloor \frac{n}{2} \right\rfloor, -\left\lfloor \frac{m-1}{2} \right\rfloor \leq l \leq \left\lfloor \frac{m}{2} \right\rfloor \right\}$$

and $\lfloor x \rfloor$ refers to the integer part of x (floor operator).

The local mean of the Roberts gradient norm $G(i,j)$ and the local mean of luminance $S(i,j)$ in a $[n \times m]$ neighborhood of pixels $A(i,j)$ can be written as follows:

$$(3) \quad S(i, j) = \frac{1}{mn} \sum_{k=p(n)}^{q(n)} \sum_{l=p(m)}^{q(m)} A(i+k, j+l) \quad \text{and} \quad G(i, j) = \frac{1}{mn} \sum_{k=p(n)}^{q(n)} \sum_{l=p(m)}^{q(m)} g(i+k, j+l)$$

with

$$p(n) = -\left\lfloor \frac{n-1}{2} \right\rfloor, \quad q(n) = \left\lfloor \frac{n}{2} \right\rfloor, \quad \text{and } g(i,j) \text{ is the Roberts gradient norm of the pixel } A(i,j).$$

SEGMENTATION STEP

The segmentation step is performed using pixel-wise classification. During this phase, each pixel is classified into one of the five classes described above.

Since we selected the features using a kernel-based method, it was natural and consistent to use the same approach for the segmentation step. However, the potential complexity of the method in high dimensional space and its dependence on unknown a priori probabilities lead us to study a simpler hyperrectangle based method which gave satisfying results in similar problems (Miteran et al., 1997).

Estimation of probability density functions using Parzen Kernel

The probability density function of each class is estimated with the classical Parzen estimator which is defined as : (Duda and Hart, 1973):

$$(4) \quad p(x_0) = \frac{1}{nh^d} \sum_{j=1}^n F\left(\frac{x_0 - x_j}{h}\right)$$

where n is the number of samples, h is the Parzen coefficient (the higher h is, the stronger the smoothing is), d is the dimension of the features space (in this case $d=3$). x_i is the sample i , and $F(u)$ is the Parzen or kernel function, which must satisfy the following conditions :

$$(5) \quad \int_{-\infty}^{+\infty} F(u) du = 1 \quad \text{and} \quad \forall u \quad F(u) \geq 0$$

In order to take into account the eventual fluctuations of data, we have chosen one of the kernels commonly used in the literature: a three dimensional gaussian. Due to the finite dimension of the features' space (each feature is normalised and coded using a byte for the real-time implementation), we have chosen to consider the gaussian function as being negligible beyond 3σ (standard deviation). So the h coefficient is equal to 3σ , we obtain the following function $F(u)$:

$$(6) \quad F(u) = \begin{cases} ae^{-\frac{u^2}{2\sigma^2}} & \text{if } |u| \leq 3\sigma \\ 0 & \text{else} \end{cases}$$

and the coefficient a is set to satisfy the conditions defined above. This kernel was used in a one-dimensional space for feature selection, and in a three-dimensional space for the learning and decision phase.

We obtained $P(x|C_i)$, the class conditional probability density for each class C_i , applying Parzen estimator with function $F(u)$ on the aforementioned learning set. Then, the Bayes decision rule is applied considering all prior probabilities of classes being equal. In fact we do not have any information about these a priori probabilities. We assume that the user will be able to establish the a priori $P(C_i)$ and $P(C_i|x)$ accordingly. For minimum error rate, we select the category most frequently represented within the cell defined by h . If there are enough samples and if the cell is sufficiently small, it can be shown that this will yield performance approaching the best possible (Duda and Hart, 1973). The value of the coefficient sigma for F is about 4. The h coefficient has a value of 12.

To ensure the convergence of the Parzen estimator, Fukunaga (1972) proposes that the change of the number of samples p implies a change of the value of h according to the following expression :

$$(7) \quad h = h(p) = h_0 p^{-\alpha/d} \quad 0 < \alpha < 1$$

Usually, α is a constant which value equals 1/2 and h_0 is a scale factor. After having created a decision space according to the previous method, it is possible to classify each pixel (low level classification) of new untrained images of pieces. This method is applicable in our case since the classifier operates in a low dimensional (3D) space.

Hyperrectangle based method : local constraint determination and decision phase

This method divides the attribute space into a set of hyperrectangles for which simple comparators may easily satisfy the membership condition. This hyperrectangle method belongs to the same family as the NGE algorithm, described in (Salzberg, 1991), whose performance was compared to the k-nn method by Wetschereck and Dietterich (1995). The performance of our own implementation was studied in (Miteran et al., 1994). These studies show that, although the division of the feature space is simple, the performance in terms of classification rate is similar to the k-nn method, and mainly significantly faster during the decision phase. Moreover, it has been shown that the method possesses a good generalization power and then works well when the sampling is poor.

This step of the training phase which is similar to the first step of the Parzen method consists in collecting the set $Sp=(s_1, s_2, \dots, s_p)$ of the most representative samples from the various classes and associating a local constraint (hyperrectangle) $H(s_i)$ to each sample s_i , defined by a feature vector \mathbf{x} in an d dimensional space and its corresponding class $C(s_i)$: $\mathbf{x}=(x_1, x_2, \dots, x_d)^T$. The hyperrectangle construction definition ensures that it cannot contain any sample of opposite classes.

The decision phase consists in allocating a class to a new attribute vector. The membership of a new feature value x_k to a given interval I_{ik} (i^{th} hyperrectangle and k^{th} feature) is easily verified by controlling the two following conditions : $(x_k > a_{ik})$ and $(x_k < b_{ik})$, where a_{ik} and b_{ik} are respectively the lower and upper limits of each polytope or hyperrectangle. Therefore, the verification of the membership of a unknown vector \mathbf{x} to a class C_p results in a set of comparisons done simultaneously, on each feature, for every hyperrectangle of class C_p . The resulting decision function is:

$$(8) \quad C(\mathbf{x}) = C_p \Leftrightarrow \sum_{i=1}^{i=Nh} \prod_{k=1}^{k=d} ((x_k > a_{ik}) \cdot (x_k < b_{ik})) \text{ is true}$$

Nh equal to the number of hyperrectangle after the merging phase. This method is easy to use, and can be implemented for real time classification, using hardware (Miteran et al., 1997) or software optimisation (Geveaux, 2000).

Comparison of the behavior of both classifiers

Figure 5 shows a part of the obtained decision space, which has been built according to the conditions described previously.

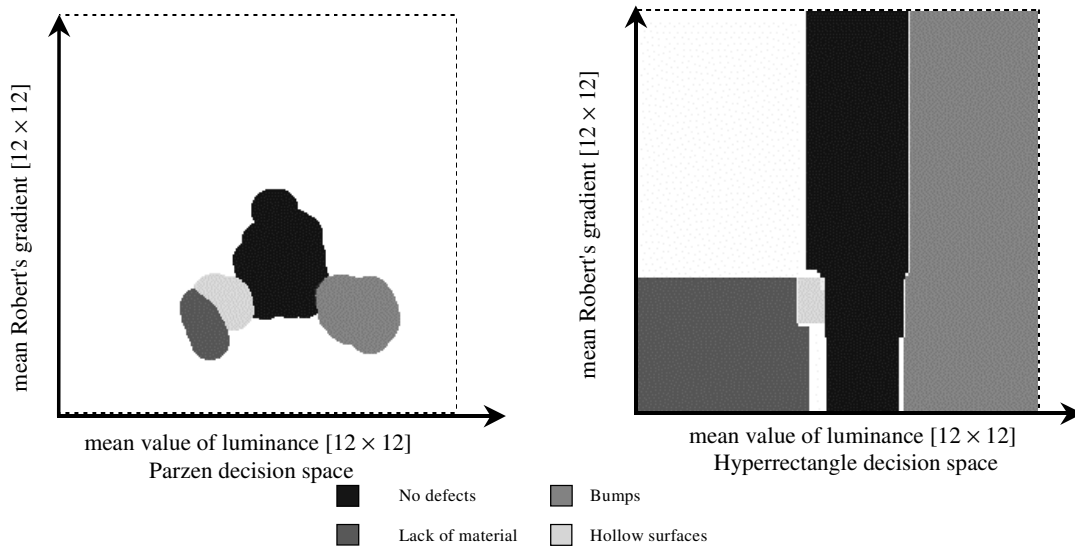


Figure 5 Cut of the obtained features space along the contrast [12x12] axis at the contrast value 145 with the Parzen classifier (left) and hyperrectangle classifier (right) (Smooth surfaces are located under the contrast value 145).

One can see that boundaries of classes are well drawn in the case of Parzen. The hyperrectangle method separates class by planar boundaries orthogonal one of the coordinate axes. These phenomena are typical of these two classifiers. Thus in the first case, borderline anomalies are better classified than with hyperrectangles. Nevertheless, the hyperrectangle method creates a generalized decision space, which allows good behavior in case of a poor training phase, unlike the Parzen method.

Furthermore in the training phase, the Parzen method deals with ambiguous samples (the same sample in the features' space belongs to several classes), unlike the hyperrectangle method which is a geometrical method and does not take into account probability densities. This problem could be solved by pre-processing the training data before the set of hyperrectangles computation.

We present in Figure 6 some examples of image segmentation using the methods described above. We show both a positive results (well classified parts) as well as negative results (incorrectly classified parts) to illustrate the limits of our method, and sometimes the difficulty in choosing the correct class even for an human expert.

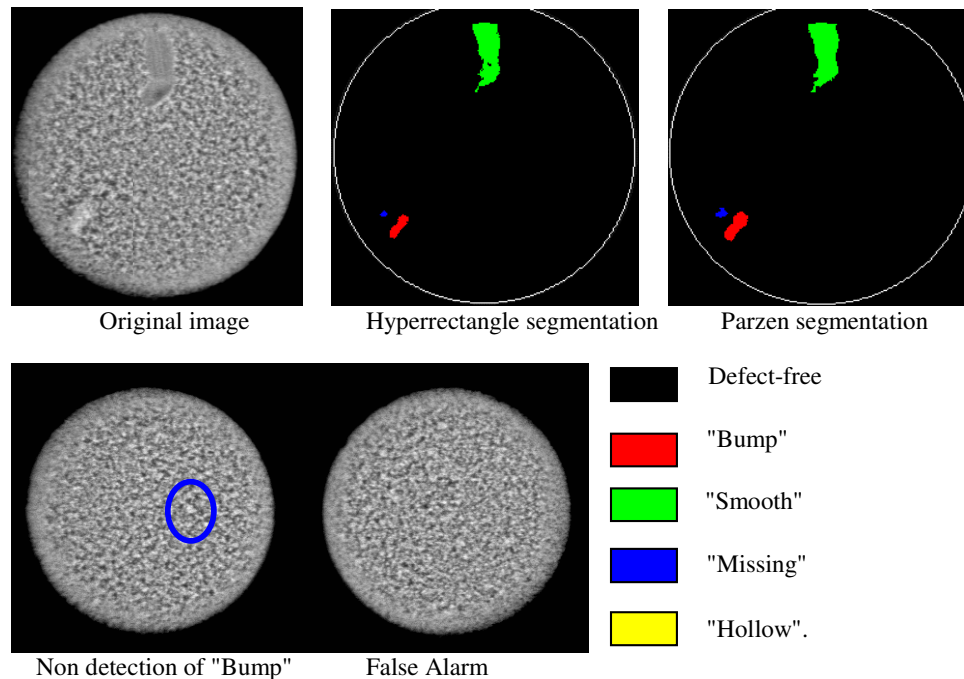


Figure 6 : Examples of segmentation results

It is clear that the defect shape is better defined using the kernel-based method than using the hyperrectangle one. However, the results are very similar in term of global classification rate. One can see moreover that the non-detected "Bump" is here so small that it is difficult to detect it even using a binocular lens. The false alarm, here, is a consequence of a higher level of texture on the right side of the image, which can be seen as a set of small bumps. To avoid this kind of false alarm, it could be interesting to adapt the feature value to the global texture measurement (Geveaux, 2000).

CATHODE CLASSIFICATION : EXPERIMENTS AND RESULTS

Definition of a test set

In order to characterize the performance of our automatic control, we used the test set of 420 industrial parts defined in the first section of this paper. This set contains 112 defect-free parts, and 308 defective parts. The choice has been made as representative of the real production in terms of defect size and appearance. The a priori probability of each class is supposed unknown, which is a disadvantage for the Parzen method.

Processed area definition and circularity control

We define the area to be processed in the image using the measurement of the part gravity center and an elliptic mask using this center and a measurement made in each quadrant oriented 45° from the image axis. However, some anomalies present on the border of the part induces some classification error. We developed then a secondary

control, defining a circular sampling around the part, and a filter allowing detecting anomalies on the border. An example of this detection is presented on Figure 7.

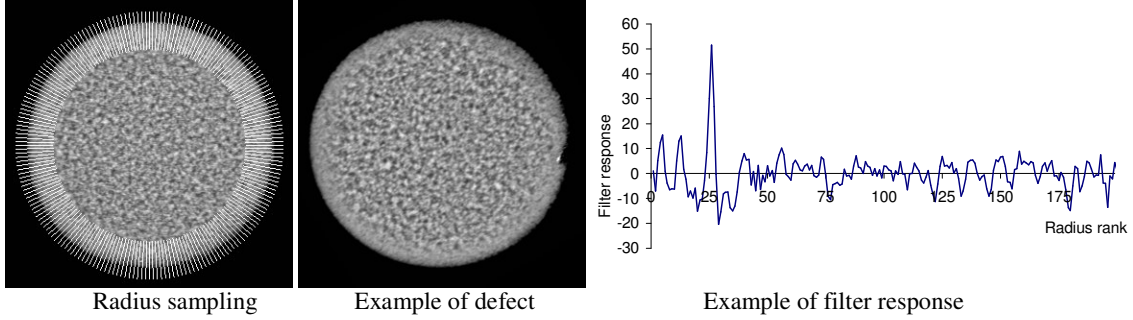


Figure 7 : Circularity control

The filter T_n is made of a low pass component, filtering the potential eccentricity of the texture on the part, a high-pass component, allowing detection of small anomalies, and a regularization term, which is adapted to the shape of the defect to be detected. Defining L_i as a i^{th} radius of the shape, $T_n(i)$ is defined by :

$$(9) \quad T_n(i) = \sum_{j=-1}^1 (L_{i+j} - M_{(i+j,n)})$$

with

$$(10) \quad M_{(i,n)} = \frac{1}{2n+1} \sum_{j=-n}^n L_{i+j}$$

Thus, the transfer function of T_n can be written as :

$$(11) \quad T_n(z) = \frac{1}{12n+6} (z+1+z^{-1}) \cdot (-z+2-z^{-1}) \cdot \left(n(n+1) + \sum_{k=1}^n (n-k)(n-k+1)(z^k + z^{-k}) \right)$$

It has been shown by Geveaux (2000) that the best value of n is 25 for our application. The final threshold is fixed using the training set defined above. The use of such a filter improves the global classification rate, avoiding artifacts due to the computation of features in a large neighborhood around each pixel to be classified. These improvements are described in the next section.

Global classification rate

During this final classification step, a high-level (or part level) decision is made, measuring the number of pixels of each class. A simple threshold is applied on these areas of each defect and on the circularity measurement. We do not need a study of same class pixels adjacency, since we suppose that a significant number of small anomalies is equivalent to a more important one.

The circularity measurement eliminates 3 False Alarm and allows detecting 3 “Bump”, 1 “Missing” and 1 “Hollow” that were not detected using the segmentation algorithms.

Table 1 shows the results obtained with the two methods. These results are obtained on the test set defined above, for a fixed ND rate.

		Non Detection			
	Total	Parzen method without circularity measurement	Parzen method with circularity measurement	Hyperrectangle without circularity measurement	Hyperrectangle with circularity measurement
"Bump"	166	9	6	8	5
"Smooth"	42	0	0	0	0
"Missing"	87	4	3	4	3
"Hollow"	13	4	3	5	4
ND (%)		5.52	3.9	5.52	3.9
False Alarm					
Defect detected on a good part	112	7	4	8	5
FA (%)		6.25	3.57	7.14	4.47

Table 1: Results obtained with both classifiers on the same set of data.

One can see that the Parzen method and Hyperrectangle method are very closed in terms of performance. The Parzen method seems to be the best compromise in our industrial application. For a similar ND rate, the FA rate of Parzen method is better (3.57%) than the FA rate of the hyperrectangle (4.47%). However, the real-time implementation of decision step using this method requires storing the complete decision space in memory (RAM). This is realistic for low dimensional feature space (less than 6). In the case of 5 features, the required memory is for example 1 Gigabyte if each feature is coded using only 6 bits. Moreover, it becomes difficult to estimate the probability density functions in each point of the space. One can note that the hyperrectangle method, in the case of medium and high dimensional feature space (more than 5), is finally more flexible for an industrial application and should be the better choice.

Real time implementation

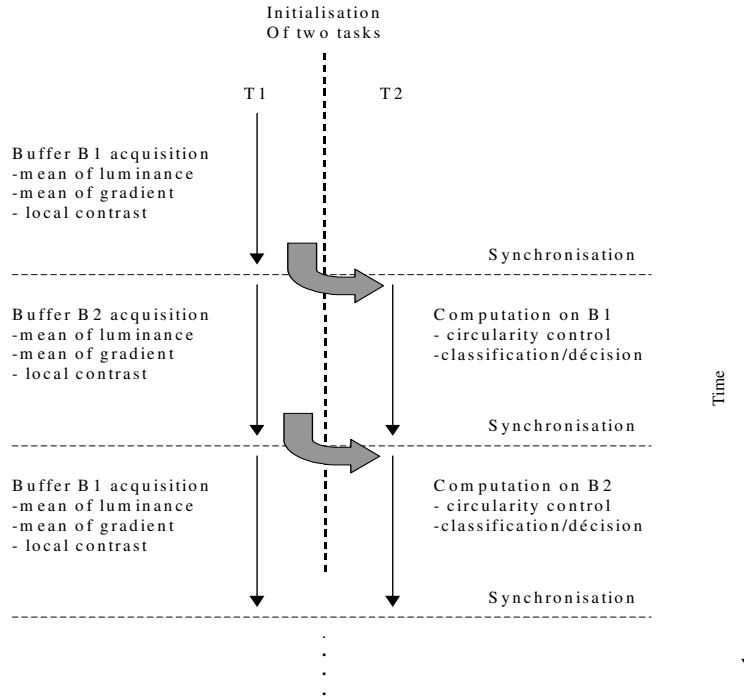


Figure 8 Multithreading computing

The description of all of the details of the implementation is not the aim of this paper. It is important to note that we study in detail different possibilities of implementation, from hardware to software. We chose finally a software implementation under Windows NT on a two-processor PC (2xPentium 500 MHz), using multithreaded computing and some optimizations for the feature extraction and the classification method (Geveaux, 2000). The different sub-tasks are distributed according to Figure 8. We present also in Table 2 some computation times obtained using different configurations.

The best results are logically obtained with two processors: all the processing is achieved in less than 50 ms.

	1xPentium 166MHz	1xPentium II 300 MHz	2xPentium II 400 MHz	2xPentium III 500 MHz
Sequential imp.	250 ms	110 ms	80 ms	60 ms
Multithreading imp.	idem	idem	50 ms	40 ms

Table 2 : Comparison of computing times

CONCLUSION AND PERSPECTIVES

We built a complete quality control system using real-time image processing. The final implementation of the inspection on the production line is under development. It includes the lighting, acquisition and processing systems described above, allowing detection of some anomalies at the rate of ten textured parts per second. The choice of the lighting system and the segmentation features used for the part classification has been made jointly and methodically

in order to optimize the detection by comparison of discrimination power of numerous features and numerous lighting systems. This method leads to the choice of parameters and illumination set-up that maximises the ability to distinguish anomalies zones from acceptable zones. It is clear that the learning phase is critical and has to be designed with care. Otherwise, the obtained results will not be significant and representative. A future work will be the generalization of the features and lighting selection method to the multidimensional case in order to allow interactions between features.

In order to obtain real time results of segmentation, we studied two methods of classification. The first one, consistent with the feature selection method, is based on the estimation of the probability density function and gives the best results, but could not be easily used in higher dimensional space. The hyperrectangle method gives results which fit the industrial constraints, and which can be used in a more general way. This method is very fast, during decision phase and during learning phase (about 5s in our case). This is an advantage for industrial applications, for which an important number of tests have to be carried out. Our future work will be adding a preprocessing step for the training data, taking account of the probability density and the a priori probability of each class before the determination of the hyperrectangle set. We have currently some interesting preliminary results using a multi-layer perceptron (Bishop, 1995) filtering learning data. These results are obtained using theoretical gaussian distributions, and we plan to apply this method using experimental data coming from a new industrial application which is under work.

REFERENCES

- D. Aluze ,C. Coulot, F. Meriaudeau, P. Gorria and C. Dumont, “*Machine vision for the control of reflecting non plane surfaces*”, Intelligent and Advanced Manufacturing, SPIE, Pittsburgh, October 1997, pp. 180-186.
- B.G.Batchelor “Automated visual inspection”, IFS 1985, pp. 13-17.
- C. M. Bishop, "Neural networks for Pattern Recognition", Oxford University Press, 1995, pp 110-230.
- J.-P.Coquerez and S. Philipp “*Analyse d’image : filtrage et segmentation*”, MASSON, Paris, 1995
- C. Coulot, S. Hemmerlin-Kohler, C. Dumont , D. Aluze and B. Lamalle, “*Simulation of lighting for an optimal defect detection by artificial vision*”, Proceedings of QCAV’97, Le Creusot, Cépaduès-Editions, 1997, pp.117-122.
- B.Dubuisson “*Diagnostic et reconnaissance des formes*,” HERMES, Paris, 1990.
- R.O. Duda and P.E. Hart, “Pattern classification and scene analysis”, Wiley, New-York, 1973, pp. 230-243.
- P. Geveaux, “Conception d’un système de détection de défauts sur surfaces texturées par traitement d’images : application au contrôle haute cadence de pièces en défilement”, PhD report, University of Burgundy, France, May 2000.
- P. Geveaux, S. Kohler, J. Miteran and F. Truchetet "Analysis of Compatibility between Lighting Devices and Descriptive Features using Parzen’s Kernel Application to Flaw Inspection by Artificial Vision", Optical Engineering, , Vol 39(12), December 2000, pp. 3165-3175.
- K. Fukunaga “*Introduction to statistical pattern recognition*”, Academic Press, New York, 1972, pp 210-211.
- W.C. Lin and M. Michael, "Experimental study of information measure and inter-intra class distance ratios on feature selection and orderings", I.E.E.E. Trans. On Systems, Man and Cybernetics, 2, 1973, pp. 172-181.
- J. Mitéran, P. Geveaux, R. Bailly and P. Gorria, “*Real time defect detection using image segmentation*”, Proceedings of IEEE-ISIE 97, Guimares, Portugal, July 1997, pp. 713-716.
- J. Mitéran, P. Gorria and M. Robert, "Classification géométrique par polytopes de contraintes. Performances et intégration", Traitement du Signal, Vol 11, n° 5, 1994, pp. 393-408.
- S. Salzberg, “*A nearest hyperrectangle learning method*”. Machine Learning, 6, 1991, pp 251-276.
- M .Unser “*Local linear transforms for texture measurements*”, Signal Processing 11, 1986, pp. 61-79.
- V. Vapnik, "Statistical Learning Theory", 1998, pp. 545-567.
- D. Wettschereck and T. Dietterich: “An Experimental Comparison of the Nearest-Neighbor and Nearest-Hyperrectangle Algorithms”. Machine Learning 19 (1,1995), pp. 5-27.